Dihydrogen Bonding under High Pressure: A Raman Study of BH_3NH_3 Molecular Crystal

Radu Custelcean* and Zbigniew A. Dreger

Institute for Shock Physics, Washington State University, Pullman, Washington 99164-2816

Received: May 8, 2003; In Final Form: July 3, 2003

The effects of high pressures (up to 40 kbar) on the dihydrogen-bonded BH_3NH_3 molecular crystal were investigated using Raman spectroscopy in diamond and moissanite anvil cells. The stretching mode frequencies of the NH_3 proton donor groups exhibited moderate red shifts with increasing pressures, as found in many conventional hydrogen-bonded systems of weak to medium strength. The stretching modes corresponding to the BH_3 proton acceptor group, on the other hand, showed large blue shifts with increasing pressure, which, however, are not related to the changes in the N−H···H−B interactions. The BH_3NH_3 crystals undergo a pressure-induced disorder−order phase transition around 8 kbar, which is facilitated by the presence of dihydrogen bonds.

I. Introduction

Molecular crystals are soft, highly compressible solids, composed of discrete molecules held together by noncovalent interactions such as van der Waals, charge transfer, or hydrogen bonds. This combination of strong intramolecular covalent bonds with weak intermolecular forces confers on molecular crystals unique properties that are often markedly different from those of covalent or ionic crystals. Despite significant recent efforts, our understanding of molecular solids is incipient compared to the covalent or ionic counterparts. Pressure is ideally suited to the study of molecular crystals, as small variations in the applied forces typically result in large changes in intermolecular separations, which often trigger dramatic reorganizations of crystal packing. One of the most important intermolecular interactions in molecular crystals is hydrogen bonding, and numerous studies directed toward the understanding of its behavior under high pressures have been reported.[1] Particularly, vibrational spectroscopy proved to be a practical tool for investigating the influence of pressure on hydrogen-bonded solids.[1a−i] As a general rule, the stretching modes of the A−H proton donors in A−H···B hydrogen bonds of weak to moderate strength exhibit a red shift in frequency with the increase of pressure, due to lengthening of the A−H bond as the A···B separation decreases.[1b] This is in marked contrast with the rest of the vibrational frequencies in the solid, which typically blue-shift with increasing pressures as a result of increased repulsion forces between neighboring molecules, and thus steeper potential well curvatures. However, compounds with strong, symmetrical hydrogen bonds exhibit a different behavior, with the A−H stretching modes typically shifting to higher frequencies with increasing pressures.[1c]

Recently, an unconventional type of hydrogen bonding, in which a σ M−H bond (M = Al, B, Ga, Ir, Mo, Mn, Os, Re, Ru, W) acts as the proton acceptor, has been the subject of numerous investigations.[2] Like conventional hydrogen bonding, this proton−hydride interaction, or dihydrogen bonding, is mostly electrostatic in nature. With interaction energies of 1−7 kcal/mol, dihydrogen bonding is comparable with moderately strong conventional hydrogen bonding. Geometrically, it is characterized by short H···H contact distances (1.7−2.2 Å) and strongly bent AH···H−M angles (90−135°). Its strong directionality allows dihydrogen bonding, like conventional hydrogen bonding, to exert considerable influence on the crystal packing of molecular crystals.[3]

The borane−ammonia complex, BH_3NH_3 (**1**), is perhaps the most studied compound with dihydrogen bonding abilities.[4] It exhibits multiple N−H···H−B intermolecular interactions in the crystalline state (Figure 1), with the shortest H−H contact distance measuring 2.02 Å.[4d] The strength of these dihydrogen bonds was estimated around 6−7 kcal/mol, from theoretical calculations on the $(BH_3NH_3)_2$ dimer.[5] It was proposed that dihydrogen bonding in **1** could account for much of its strikingly higher melting point (+104 °C) relative to the isoelectronic ethane (−181 °C).[2b]

The BH_3NH_3 complex also represents a prototypical donor−acceptor system, formed by the donation of the lone pair of NH_3 to the empty 2p orbital of BH_3.[6] The resulting B−N dative bond has a dissociation energy of about 31 kcal/mol,[7] which is midway between typical values found in van der Waals and covalent interactions. However, theoretical calculations indicated that BH_3NH_3 is better described as a strong van der Waals complex rather than a covalently bonded molecule.[6b] A characteristic feature of this donor−acceptor complex is that the B−N dative bond is significantly shorter in the solid state (1.58 Å) compared to the gas phase (1.67 Å), apparently as a result of cooperative dipole−dipole interactions in the crystal.[4a,b] These structural characteristics make BH_3NH_3 a particularly interesting case of molecular crystal to be studied under high pressure. Herein we report the effects of pressures up to 40 kbar on the crystalline BH_3NH_3, which represents the first comprehensive high-pressure study of a dihydrogen-bonded solid.[8] We show the spectroscopic behavior of dihydrogen bonds under hydrostatic compression is qualitatively similar to that found in moderately strong conventional hydrogen bonds. We also report a pressure-induced disorder−order phase transition in **1**, which is similar to that previously reported in low-temperature studies. The analogous complexes $BH_3N(CH_3)_3$ (**2**), and $B(Ph)_3NH_3$ (**3**), with no dihydrogen bonds, were also analyzed to assess the role played by dihydrogen bonding in the observed pressure-induced transformations in BH_3NH_3.

* Corresponding author. E-mail: custelce@wsu.edu.

10.1021/jp035267+ CCC: $25.00
Published on Web 08/05/2003

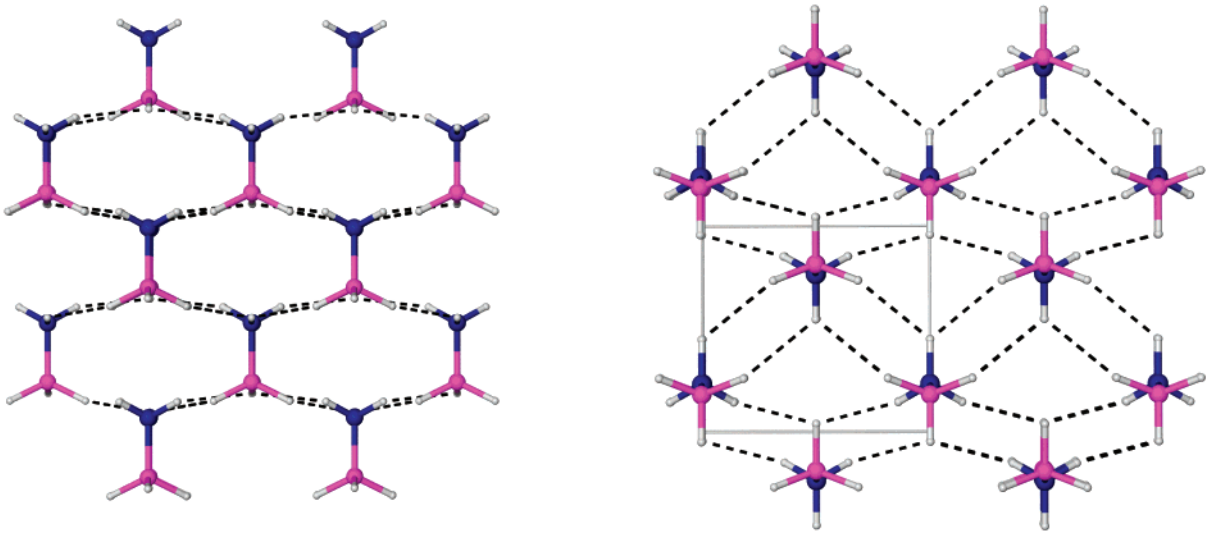

Figure 1. Low-temperature (orthorhombic) crystal structure of BH_3NH_3. Left: view along crystallographic *b* axis. Right: view along crystallographic *c* axis. N, B, and H atoms are depicted in blue, purple, and gray, respectively. The dihydrogen bonds are delineated by dashed lines. The unit cell is demarcated by gray lines.

II. Experimental Methods

The borane−ammonia (90%) and borane−trimethylamine (97%) complexes were purchased from Aldrich, and the triphenylboron−ammonia complex (98%) was purchased from Strem Chemicals. BH_3NH_3 was further purified by recrystallization from diethyl ether. Polycrystalline samples were loaded in modified Merrill-Bassett type diamond- or moissanite-anvil-cells. Stainless steel or Inconel gaskets with a 0.2 mm central hole were used for the sample compartment. Mineral oil was used as the pressure-transmitting medium in all experiments. The National Bureau of Standards (NBS) ruby calibration method was applied for monitoring the pressure.[9] Thus, a small chip of ruby was placed inside the gasket aperture along with the sample, and was excited with a 532 nm line from a diode-pumped solid-state laser (DPSSL-Crystalaser). The ruby fluorescence was dispersed by a 0.22 m double spectrometer (Spex 1680) and detected by an air-cooled CCD (Princeton Instruments). The pressure experienced by the crystal was monitored with an estimated accuracy of ±0.5 kbar, by measuring the frequency shift of the ruby R_1 fluorescence line. The virtually constant widths and separations of the R_1 and R_2 lines maintained during these measurements confirmed the hydrostatic conditions throughout our experiments.

The 514.5 nm line from an Ar-ion laser (Innova 90-Coherent) was employed for the Raman excitation. The scattered signal was collected in a backscattering geometry and analyzed by a 0.6 m triple spectrometer (Spex 1877) and a liquid nitrogen-cooled CCD (Princeton Instruments). The estimated resolution was about 1 cm^{-1}. All experiments were carried out at room temperature.

III. Results

Table 1 presents the fundamental vibrational frequencies of **1**, observed in our Raman experiment at ambient pressure. The mode assignment was done by comparison with the reported infrared values for **1** in an Ar matrix,[10] ether solution,[11] or KBr.[12] The agreement between our data and the reported infrared data is generally good. One notable difference is in the N−H and B−H stretching modes found in the crystal, which are significantly red-shifted compared to the matrix-isolated molecule, as a result of dihydrogen bonding in the solid state. Thus, the symmetric and asymmetric N−H stretching modes are red-shifted by 82 and 70 cm^{-1}, respectively, in the crystal. The analogous B−H modes are red-shifted by 60 and 40 cm^{-1}, respectively. There has been a long controversy on the assignment of the B−N stretching frequency of BH_3NH_3. This mode was originally assigned to 785 cm^{-1} (ether solution) by Taylor[11] and confirmed by Sawodny (KBr),[12] who found a similar value of 776 cm^{-1}. Smith et al. later reassigned it to 968 cm^{-1} on the basis of their infrared study in Ar matrix.[10] We observed the B−N stretching mode at 782 cm^{-1}, which confirms the original assignment. We also observed a weak peak at 798 cm^{-1}, which we assigned to the B−N stretching mode of the $^{10}BH_3NH_3$ isotopomer, on the basis of ab initio calculations[13] at the B3LYP/aug-cc-PVTZ level, which predicts a difference of 18 cm^{-1} between the ^{11}B−N and ^{10}B−N stretching modes.

TABLE 1: Fundamental Vibrational Frequencies for BH_3NH_3

		frequencies (cm^{-1})			
mode	sym	molecule (Ar/ether)[a]	KBr[b]	crystal[c]	assignment
ν_1	A_1	3337	3245	3255	sym N−H stretch
ν_2	A_1	2340	2277	2280	sym B−H stretch
ν_3	A_1	1343	1374	1375	sym N−H bend
ν_4	A_1	1175	1026	1158	sym B−H bend
ν_5	A_1	968/785	776	782	^{11}B−N stretch
ν_5'	A_1			798	^{10}B−N stretch
ν_6	A_2				B−N torsion[d]
ν_7	E	3386	3312	3316	asym N−H stretch
ν_8	E	2415	2316	2375	asym B−H stretch
ν_9	E	1608	1597	1596	asym N−H bend
ν_{10}	E	1186	1165	1185	asym B−H bend
ν_{11}	E	1052	1058	1066	asym N−H + B−H rock
ν_{12}	E	603	715	726	asym N−H + B−H rock

[a] References 10 and 11. [b] Reference 12. [c] This work. [d] Not observed.

Figures 2 and 3 illustrate the evolution of the most important Raman modes with pressure. The N−H stretching modes (Figures 2a and 3a) shift to lower frequencies, whereas the B−H (Figures 2b and 3b) and B−N (Figures 2c and 3c) stretching modes shift to higher frequencies with increasing pressures.

There is an evident phase transition around 8 kbar, as indicated by the significant narrowing of the peaks, as well as by the splitting of the modes with *E* symmetry. The splitting of the asymmetric B−H mode, however, could only be resolved above 25 kbar, due to the initial close proximity of the resulting

TABLE 2: Pressure Coefficients of the External and Internal Modes of BH_3NH_3

	$\Delta\nu/\Delta P$ (cm^{-1}/kbar)[a]			$(1/\nu)(\Delta\nu/\Delta P) \times 10^2$ (%/kbar)		
mode	phase I	phase II		phase I	phase II	
lattice		0.66			0.38	
^{11}B−N stretch	2.47	0.99		0.31	0.12	
^{10}B−N stretch	2.40	1.07		0.30	0.13	
sym B−H stretch	1.49	0.89		0.07	0.04	
asym B−H stretch	1.94	1.06[b]		0.08	0.04[b]	
		1.81[c]	0.74[c]		0.07[c]	0.03[c]
sym N−H stretch	−0.65	−0.27		−0.02	−0.008	
asym N−H stretch	−0.36	−0.29	−0.47	−0.01	−0.009	−0.014

[a] Pressure coefficients were estimated by least-squares fitting of the experimental data to linear equations. [b] Pressure coefficients before peak splitting. [c] Pressure coefficients after peak splitting.

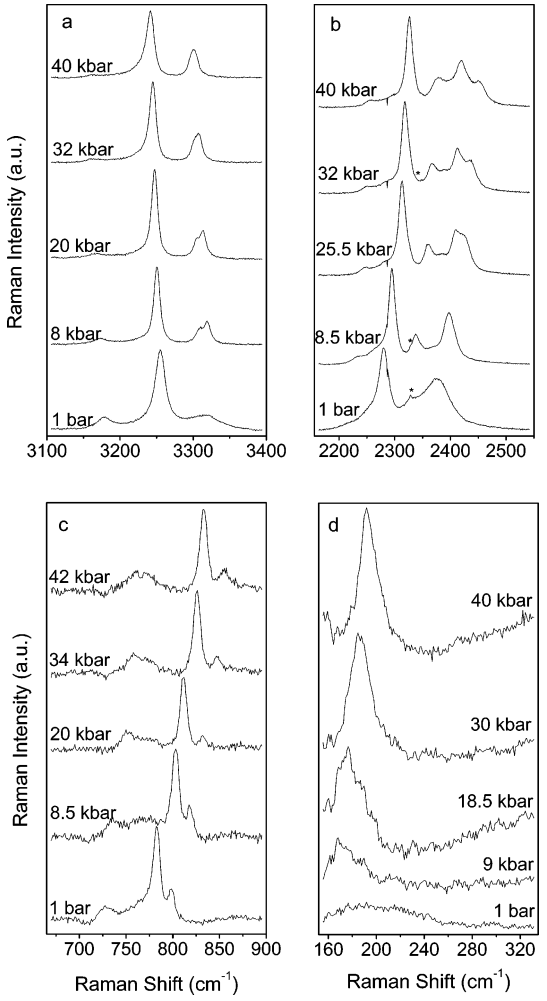

Figure 2. Evolution of Raman spectra of **1** with pressure. (a) N−H stretching modes. (b) B−H stretching modes. The asterisks indicate peaks from moissanite. (c) B−N stretching modes. (d) Lattice mode.

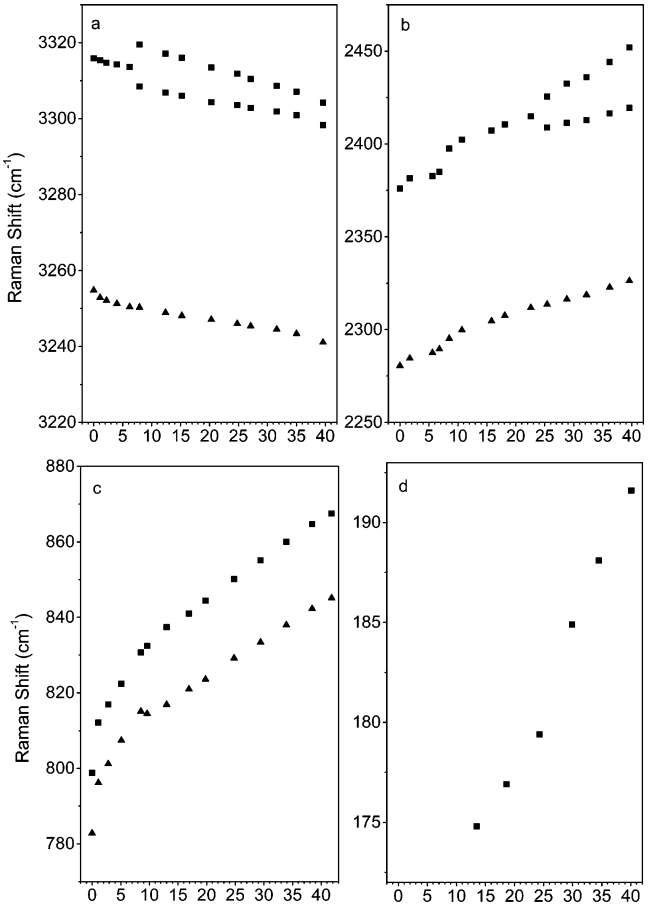

Figure 3. Pressure-induced shifts of selected Raman modes of **1**. (a) Symmetric (▲) and asymmetric (■) N−H stretching modes. (b) Symmetric (▲) and asymmetric (■) B−H stretching modes. (c) ^{11}B−N (▲) and ^{10}B−N (■) stretching modes. (d) Lattice mode.

peaks. The splitting of the asymmetric N−H stretching mode, on the other hand, could be initially resolved, but the difference in frequency between the two resulting peaks decreased with pressure, until the peaks coalesced around 40 kbar. The phase transition was also apparent by the development of a peak around 175 cm^{-1}, assigned to a lattice vibration mode, which became more pronounced and shifted to higher frequencies with increasing pressures (Figure 2d). All pressure-induced transformations were reversible, although some hysteresis was observed upon pressure unloading.

Table 2 lists the calculated pressure coefficients ($\Delta\nu/\Delta P$, cm^{-1}/kbar) for the monitored peaks in the two phases, obtained by least-squares fitting of the experimental data to linear equations. For direct comparison, pressure coefficients normalized to the corresponding peak frequencies are also listed.

As a general trend, the pressure coefficients are noticeably larger for phase I compared to phase II. As expected, the normalized pressure coefficient of the lattice mode (0.38%/kbar) is significantly larger than the corresponding value of the B−H internal modes (0.04%/kbar). The stretching vibration mode of the dative B−N bond shifts by 0.12%/kbar, which is an intermediate value between the corresponding values for the internal and external modes. The N−H stretching vibration modes show negative pressure dependences, with normalized pressure coefficients around −0.01%/kbar.

To assess the role played by dihydrogen bonds in the observed phase transition and the blue shift of the B−H stretching

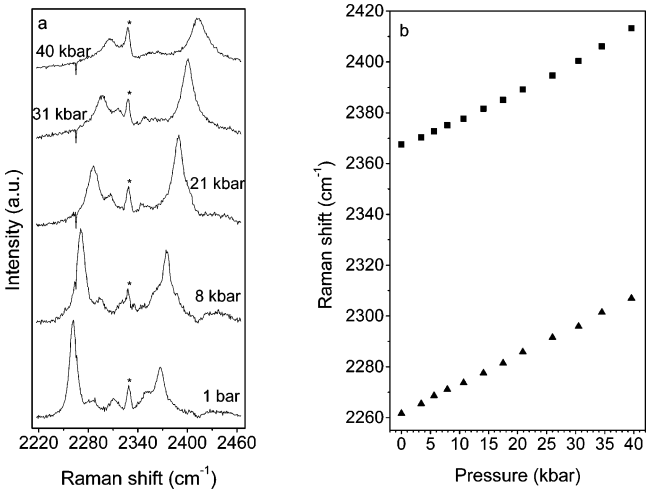

Figure 4. (a) Evolution of the B−H stretching modes of **2** with pressure. The asterisks indicate peaks from moissanite. (b) Pressure-induced shifts of the symmetric (▲) and asymmetric (■) B−H stretching modes.

frequencies in **1**, we also measured the effects of pressure on the Raman spectra of the analogous complex $BH_3N(CH_3)_3$ (**2**), in which the dihydrogen bonds were shut off by substitution of the N−H protonic hydrogens by Me groups. The symmetric and asymmetric B−H stretching modes of **2** were located at 2262 and 2368 cm^{-1} at ambient conditions. Their evolution with pressure is depicted in Figure 4.

Unlike **1**, complex **2** did not undergo any pressure-induced phase transition. Instead, the monitored peaks gradually lost intensity and became broader (Figure 4a), which suggests progressive loss of order with increasing pressures.

Another control experiment was carried out to estimate the role played by dihydrogen bonding in the observed red shifts of the N−H stretching modes in **1**. For this purpose, the dihydrogen bonds were shut off by substitution of the hydridic hydrogens with Ph groups. The corresponding complex, $B(Ph)_3NH_3$ (**3**), exhibits a Raman N−H stretching mode of weak intensity at 3417 cm^{-1}, which, however, is virtually unaffected by pressures of up to 40 kbar.

IV. Discussion

The isolated BH_3NH_3 molecule has C_{3v} symmetry and exhibits 18 fundamental vibrations: $\Gamma = 5A_1 + A_2 + 6E$ (Table 1). There are two known crystalline phases of **1**.[14] At room temperature it crystallizes in a body-centered tetragonal system, space group *I*4*mm*, with the molecules sitting on the 4-fold axes. This phase is highly disordered, as the BH_3 and NH_3 groups undergo a 3-fold rotation about the B−N bond, so that each H atom occupies three available equilibrium positions with equal probability. Additionally, the whole molecule rotates about the 4-fold crystallographic axis, so overall the BH_3 and NH_3 groups execute twelve-fold reorientations.[15] This orientational disorder confers a high degree of plasticity on the room-temperature crystalline phase of **1**. Upon cooling below 225 K, these plastic crystals undergo a first-order−disorder-order phase transition to an orthorhombic phase with $Pmn2_1$ space group symmetry.[14] In this phase, the BH_3 and NH_3 groups still undergo uncorrelated 3-fold rotations about the B−N bond, but the BH_3NH_3 molecules are now locked in an extended dihydrogen-bonded network (Figure 1).[15] Because in the low-temperature phase the molecules lie on the crystallographic mirror plane and thus have C_s site symmetry ($\Gamma = 11A' + 7A''$), splitting of the double-degenerate E modes is expected upon phase transition.

The disorder−order phase transition in **1** can also be induced by pressure, as demonstrated by the splitting of the asymmetric N−H and B−H stretching modes (Figure 2), as well as by the changes in the pressure coefficients around 8 kbar (Figure 3). The disorder−order phase transition was also evidenced by the appearance of a lattice mode around 175 cm^{-1}, which was absent in the original disordered phase. Our results are qualitatively and quantitatively different from those recently published by Trudel and Gilson, who found two pressure-induced phase transitions in **1**, at 5 and 14 kbar.[8] The discrepancy may originate in the different experimental conditions present in the two studies. While we used mineral oil as a pressure-transmitting medium to ensure hydrostatic conditions, no information related to the pressure-transmitting medium was provided in the other study, which makes the comparison difficult. It is known that under nonhydrostatic conditions the sample may experience pressure gradients, which may result in different transition pressures compared to those found under hydrostatic conditions.[16]

An important question is what role does dihydrogen bonding play in the observed disorder−order phase transition in **1**? To address this question, we measured the effects of pressure on the similar donor−acceptor complex $BH_3N(CH_3)_3$ (**2**), which, however, cannot form dihydrogen bonds due to the lack of protonic hydrogens. Like **1**, complex **2** crystallizes in a plastic phase at room temperature, which suggests the occurrence of similar orientational disorder. Unlike in **1**, however, no pressure-induced phase transition was observed in **2**, up to 40 kbar (Figure 4). The decrease in intensity and broadening of the Raman peaks of **2** indicate instead further decrease of order with pressure. These results strongly suggest that dihydrogen bonding has a decisive role in the observed pressure-induced phase transition in **1**. At sufficiently high pressures, these highly directional N−H···H−B interactions become sufficiently strong to efficiently lock the BH_3NH_3 molecules in a three-dimensional ordered network.

The N−H stretching mode frequencies in **1** undergo a moderate red shift with increasing pressures (about −14 cm^{-1}/40 kbar), suggesting that dihydrogen bonding behaves similarly at high pressure as conventional hydrogen bonding, although the magnitude of the shift is somewhat smaller than that found for typical hydrogen-bonded solids.[1] The interpretation of the observed frequency shifts in **1** is unfortunately complicated by the occurrence of other pressure-induced structural modifications, which may directly influence the N−H and B−H stretching modes. For instance, the shortening of the dative B−N bond with pressure is expected to increase the sp^3 character of both the B and N atoms, as they become more pyramidalized, which in turn should red-shift the corresponding B−H and N−H stretching modes. It is therefore not clear to what extent are the observed N−H shifts in **1** related to changes in dihydrogen bonding upon compression. To estimate the intrinsic shifts of the N−H and B−H stretching modes associated with shortening of the B−N bond with pressure, we performed ab initio calculations at the B3LYP/6-31G* level on the isolated BH_3-NH_3 molecule. Thus, we gradually decreased the B−N bond length until the calculated shift of the B−N stretching mode was comparable with that found experimentally. We found that by shortening the B−N bond by 1.4% of its original value in the crystal resulted in blue-shifting of the corresponding B−N stretching mode by 51 cm^{-1}, which is similar with the shift observed in our experiment. In turn, the symmetric and asymmetric N−H stretching modes shifted by −5 and −8 cm^{-1}, respectively, whereas the analogous B−H modes shifted by −3

and -7 cm^{-1}. The extent of the inherent N−H red shift caused by shortening of the B−N bond length was also indirectly estimated from a control experiment with the analogous complex $B(Ph)_3NH_3$ (**3**) with no dihydrogen bonds. The N−H stretching mode in **3**, observed at 3417 cm^{-1} at ambient conditions, was virtually unaffected by pressures of up to 40 kbar. This result, together with the theoretical calculations, suggest that the shortening of the B−N dative bond has negligible effects on the N−H and B−H stretching modes. We therefore conclude that the observed shifts of the N−H mode frequencies in **1** are mainly due to strengthening of dihydrogen bonding with pressure.

In direct contrast to the stretching modes of the NH_3 proton donor group, the corresponding modes of the BH_3 proton acceptor group in **1** exhibited large blue shifts with pressure (46 cm^{-1}/40 kbar for sym B−H). For comparison, the analogous B−H mode of complex **2**, with no dihydrogen bonds, exhibited a very similar shift (45 cm^{-1}/40 kbar), which suggests that dihydrogen bonding has virtually no influence on the pressure-induced shift of the B−H stretching mode in **1**. This conclusion is somewhat surprising, as one might expect that strengthening of the N−H···H−B interactions with pressure would result in weakening of the B−H bond, and thus red-shifting of the corresponding B−H stretching modes. Further in-depth theoretical calculations, including the electron density redistribution in **1** with pressure, are necessary to rationalize our experimental findings.

A final note on the observed pressure-induced shift of the B−N stretching mode in **1** is warranted. The dative character of the B−N bond places it at the midpoint between van der Waals and covalent interactions. As shown in Table 2, the B−N bond responds accordingly to pressure. Thus, the B−N stretching mode blue-shifts by 0.12%/kbar in phase II, a relative shift that is 3 times larger than the corresponding shift of 0.04%/kbar for the B−H covalent bond, and about 3 times smaller than the corresponding value of 0.38%/kbar for the observed external mode.

V. Conclusions

The high-pressure effects on the dihydrogen-bonded BH_3-NH_3 molecular crystal have been investigated by Raman spectroscopy. We observed a pressure-induced disorder−order phase transition around 8 kbar, similar to that previously reported in low-temperature studies. This result is different from the recently published high-pressure study of **1**, which found two phase transitions at 5 and 14 kbar. The discrepancy could originate in the difference in the hydrostatic conditions applied in the two studies. Dihydrogen bonding appears to play a critical role in the observed disorder−order phase transition, as no such transformation was found in the similar complex **2**, with no dihydrogen bonds. The N−H stretching modes of **1** shift to lower frequencies with pressure, as a result of strengthening of the dihydrogen bonds. The corresponding B−H modes, on the other hand, undergo blue shifts with pressure, which, however, are not related to the changes in the N−H···H−B interactions. The B−N stretching mode shows a pressure behavior that is intermediate between those found for internal and external modes, in accord with the character of the B−N dative bond, which is midway between covalent and van der Waals.

Acknowledgment. This work was supported by ONR grant N000149310369 and DOE grant DEFG0397SF21388. We thank Prof. Yogendra M. Gupta for his support and encouragement of this study.

References and Notes

(1) (a) Moon, S. H.; Drickamer, H. G. *J. Chem. Phys.* **1974**, *61*, 48. (b) Hamann, S. D.; Linton, M. *Aust. J. Chem.* **1975**, *28*, 2567. (c) Hamann, S. D.; Linton, M. *Aust. J. Chem.* **1976**, *29*, 479. (d) Hamann, S. D.; Linton, M. *Aust. J. Chem.* **1976**, *29*, 1641. (e) Hamann, S. D.; Linton, M. *Aust. J. Chem.* **1976**, *29*, 1825. (f) Shimizu, H.; Nagata, K.; Sasaki, S. *J. Chem. Phys.* **1988**, *89*, 2743. (g) Aoki, K.; Kakudate, Y.; Yoshida, M.; Usuba, S.; Fujiwara, S. *J. Chem. Phys.* **1989**, *91*, 2814. (h) Mammone, J. F.; Sharma, S. K.; Nicol, M. *J. Phys. Chem.* **1980**, *84*, 3130. (i) Rao, R.; Sakuntala, T.; Godwal, B. K. *Phys. Rev. B* **2002**, *65*, 054108. (j) Allan, D. R.; Clark, S. J. *Phys. Rev. B* **1999**, *60*, 6328. (k) Allan, D. R.; Clark, S. J. *Phys. Rev. Lett.* **1999**, *82*, 3464. (l) Allan, D. R.; Clark, S. J.; Brugmans, M. J. P.; Ackland, G. J.; Vos, W. L. *Phys. Rev. B* **1999**, *60*, 6328.

(2) (a) Custelcean, R.; Jackson, J. E. *Chem. Rev.* **2001**, *101*, 1963. (b) Crabtree, R. H.; Siegbhan, E. M.; Eisenstein, O.; Rheingold, A. L.; Koetzle, T. F. *Acc. Chem. Res.* **1996**, *29*, 348. (c) Calhorda, M. J. *Chem. Commun.* **2000**, 801. (d) Epstein, L. M.; Shubina, E. S. *Coord. Chem. Rev.* **2002**, *231*, 165. (e) Abdur-Rashid, K.; Morris, R. H. *Can. J. Chem.* **2001**, *79*, 964. (f) Alkorta, I.; Elguero, J.; Mo, O.; Yanez, M.; Del Bene, J. E. *J. Phys. Chem. A* **2002**, *106*, 9325.

(3) Custelcean, R.; Vlassa, M.; Jackson, J. E. *Chem. Eur. J.* **2002**, *8*, 302.

(4) (a) Dillen, J.; Verhoeven, P. *J. Phys. Chem. A* **2003**, *107*, 2570. (b) Merino, G.; Bakhmutov, V. I.; Vela, A. *J. Phys. Chem. A* **2002**, *106*, 8491. (c) Li, J. S.; Zhao, F.; Jing, F. Q. *J. Chem. Phys.* **2002**, *116*, 25. (d) Klooster, W. T.; Koetzle, T. F.; Siegbahn, P. E. M.; Richardson, T. B.; Crabtree, R. H. *J. Am. Chem. Soc.* **2000**, *121*, 6337. (e) Popelier, P. L. A. *J. Phys. Chem. A* **1998**, *102*, 1873.

(5) (a) Richardson, T. B.; de Gala, S.; Crabtree, R. H.; Siegbhan, P. E. M. *J. Am. Chem. Soc.* **1995**, *117*, 12875. (b) Cramer, C. J.; Gladfelter, W. L. *Inorg. Chem.* **1997**, *36*, 5358.

(6) (a) Horvath, V.; Kovacs, A.; Hargittai, I. *J. Phys. Chem. A* **2003**, *107*, 1197. (b) Jagielska, A.; Moszynski, R.; Piela, L. *J. Chem. Phys.* **1999**, *110*, 947. (c) Leboeuf, M.; Russo, N.; Salahub, D. R.; Toscano, M. *J. Chem. Phys.* **1995**, *103*, 7408. (d) Vijay, A.; Sathyanarayana, D. N. *Chem. Phys.* **1995**, *198*, 345. (e) Es−Sofi, A.; Serrar, C.; Ouassas, A.; Jarid, A.; Boutalib, A.; Nebot-Gil, I.; Tomas, F. *J. Phys. Chem. A* **2002**, *106*, 9065.

(7) Haaland, A. *Angew. Chem., Int. Ed. Engl.* **1989**, *28*, 992.

(8) During the preparation of this manuscript, a similar high-pressure study of BH_3NH_3 was reported (Trudel, S.; Gilson, D. F. R. *Inorg. Chem.* **2003**, *42*, 2814). This succinct report, however, does not address the role of dihydrogen bonds in the observed pressure-induced phase transition in **1**, or the effects of pressure on the donor−acceptor interaction between NH_3 and BH_3, which has a direct influence on the vibrational frequencies of these groups.

(9) Barnett, J. D.; Block, S.; Piermarini, G. J. *Rev. Sci. Instrum.* **1973**, *44*, 1.

(10) Smith, J.; Seshadri, K. S.; White, D. *J. Mol. Spectrosc.* **1973**, *45*, 327.

(11) Taylor, R. C.; Cluff, C. L. *Nature* **1958**, *182*, 390.

(12) Sawodny, W.; Goubeau, J. *Z. Phys. Chem.* **1965**, *44*, 227.

(13) Frisch, M. J.; Trucks, G. W.; Schlegel, H. B.; Scuseria, G. E.; Robb, M. A.; Cheeseman, J. R.; Zakrzewski, V. G.; Montgomery, J. A.; Stratmann, R. E.; Burant, J. C.; Dapprich, S.; Millam, A. D.; Daniels, A. D.; Kudin, K. N.; Strain, M. C.; Farkas, O.; Thomasi, J.; Barone, V.; Cossi, M.; Cammi, R.; Mennucci, B.; Pomelli, C.; Adamo, C.; Clifford, S.; Ochterski, J.; Petersson, G. A.; Ayala, P. Y.; Cui, Q.; Morokuma, K.; Malick, D. K.; Rabuck, A. D.; Raghavachari, K.; Foresman, J. B.; Cioslowski, J.; Ortiz, J. V.; Stefanov, B. B.; Liu, G.; Liashenko, A.; Piskorz, P.; Komaromi, I.; Gomperts, R.; Martin, R. L.; Fox, D. J.; Keith, T.; Al-Laham, M. A.; Peng, C. Y.; Nanayakkara, A.; Gonzalez, C.; Challacombe, M.; Gill, P. M. W.; Johnson, B. G.; Chen, W.; Wong, M. W.; Andres, J. L.; Head-Gordon, M.; Replogle, E. S.; Pople, J. A. *Gaussian98*, revision 5.2; Gaussian, Inc.: Pittsburgh, PA, 1998.

(14) Hoon, C. F.; Reynhardt, E. C. *J. Phys. C* **1983**, *16*, 6129.

(15) (a) Reynhardt, E. C.; Hoon, C. F. *J. Phys. C* **1983**, *16*, 6137. (b) Penner, G. H.; Chang, Y. C. P.; Hutzal, J. *Inorg. Chem.* **1999**, *38*, 2868.

(16) Peiris, S. M.; Pangilinan, G. I.; Russell, T. P. *J. Phys. Chem. A* **2000**, *104*, 11188.